Impairment of the autophagic flux in astrocytes intoxicatedby trimethyltin

Cinzia Fabrizi [a,1], Elena Pompili [a,1], Stefania De Vito [a], Francesca Somma [a], Angela Catizone [a], Giulia Ricci [b], Paola Lenzi [c,*], Francesco Fornai [c,d], Lorenzo Fumagalli [a]

[a] Department of Anatomy, Histology, Forensic Medicine and Orthopedics, Sapienza University, Rome, Italy
[b] Department of Experimental Medicine, Second University of Naples, Naples, Italy
[c] Department of Human Morphology and Applied Biology, Pisa, Italy
[d] I.R.C.C.S. Neuromed, Pozzilli, Italy

A B S T R A C T

Autophagy is a lysosomal catabolic route for protein aggregates and damaged organelles which in different stress conditions, such as starvation, generally improves cell survival. An impairment of this degradation pathway has been reported to occur in many neurodegenerative processes. Trimethyltin (TMT) is a potent neurotoxin present as an environmental contaminant causing tremors, seizures and learning impairment in intoxicated subjects. The present data show that in rat primary astrocytes autophagic vesicles (AVs) appeared after few hours of TMT treatment. The analysis of the autophagic flux in TMT-treated astrocytes was consistent with a block of the late stages of autophagy and was accompanied by a progressive accumulation of the microtubule associated protein light chain 3 (LC3) and of p62/SQSTM1. Interestingly, an increased immunoreactivity for p62/SQSTM1 was also observed in hippocampal astrocytes detected in brain slices of TMT-intoxicated rats. The time-lapse recordings of AVs in EGFP-mCherry-LC3B transfected astrocytes demonstrated a reduced mobility of autophagosomes after TMT exposure respect to control cells. The observed block of the autophagic flux cannot be overcome by known autophagy inducers such as rapamycin or 0.5 mM lithium. Although ineffective when used at 0.5 mM, lithium at higher concentrations (2 mM) was able to protect astrocyte cultures
from TMT toxicity. This effect correlated well with its ability to determine the phosphorylation/ inactivation of glycogen kinase synthase-3b (GSK-3b).

1. Introduction

Autophagy is an evolutionary conserved lysosomal degradation pathway which allows the turnover of long-lived, misfolded or aggregated proteins; it also provides the removal of organelles which are damaged or in excess (Levine and Kroemer, 2008). It is initiated by the formation of a phagophore which then expands forming a double-membrane vesicle, the autophagosome. On autophagic induction the microtubule associated protein light chain 3 (LC3)-I is conjugated to posphatidylethanolamine on its C-terminus to form LC3-II which binds tightly to the autophago- somal membrane (Kabeya et al., 2000). Vesicle content is then degraded when autophagosomes fuse with lysosomes giving autophagolysosomes. Autophagy is activated during starvation in order to restore intracellular nutrient supply but also after different stress conditions allowing the removal of protein aggregates or damaged organelles (for a recent review see Noda and Inagaki, 2015).

Trimethyltin chloride (TMT) belongs to a family of organotin compounds with wide industrial and agricultural applications, especially as heat stabilizers in PVC production and also as biocides. Mono-, di- and trimethyltin compounds can be detected as contaminants in fresh water, tap water, seawater, algae and fish (Fent, 1996; Mundy and Freudenrich, 2006). Leaching of organo- tins from PVC material has been proposed to be one of the principal sources of environmental contamination (Richardson and Edwards, 2009). Concerns about their toxicity have led to a worldwide ban of the most toxic species but despite these global restrictions in many countries of Europe and North America, organotin compounds are still largely used. In China, for instance, due to their wide industrial applications, organotins are found in many environmental media (Cao et al., 2009).

Organotin compounds are absorbed through inhalation, inges- tion and dermal exposure causing toxic effects on skin, eyes, respiratory system, gastrointestinal system and nervous system. In humans TMT caused predominantly clinical signs of limbic system and cerebellar dysfunction, hearing loss, and to a lesser degree, a mild sensory disturbance (Besser et al., 1987). In both humans and rodents, TMT determines the selective destruction of neurons in specific brain regions such as the olfactory bulb, hippocampus, amygdala, pyriform/enthorinal cortex, and pyramidal cells in the neocortex (Chang and Dyer, 1985; Kawada et al., 2008).

The mechanism underlying TMT selectivity is not completely known although its toxicity was reported to correlate with the expression of stannin, a transmembrane protein mainly localized to the membranes of mitochondria and other organelles (Davidson et al., 2004). In this connection, triorganotin compounds in general and TMT in particular are known to perturb mitochondrial functions leading to the inability of these organelles to synthetize ATP and subsequently to their gross swelling (Aldridge et al., 1977), to the loss of mitochondrial membrane potential and to cytochrome c release (Misiti et al., 2008). Low energy levels and cellular stress are known to inhibit mTORC1 leading to the activation of catabolic processes such as autophagy (Zoncu et al., 2011).

Our previous data indicated autophagy to be a pro-survival mechanism for neurons exposed in culture to TMT (Fabrizi et al., 2012). Thus in this paper we wanted to investigate the autophagic pathway also in TMT-intoxicated astrocytes. Astrocytes are the most numerous cells in the mammalian brain and are recognized as active players in the regulation of synaptic function, neural repair and maintenance of the blood–brain barrier (BBB) (Cabezas et al., 2014). TMT neurotoxicity is always accompanied in vivo by extensive microgliosis and astrogliosis (Haga et al., 2002; Pompili et al., 2004, 2011) and the integrity of the BBB appears early compromised in rodents following TMT administration causing a leakage of IgG in the brain parenchyma (Ceccariglia et al., 2014).

2. Materials and methods

2.1. Cell cultures and treatments

All procedures were carried out in accordance with the Italian laws and guidelines established for the care and the use of animals in research. Astrocytes were prepared from mixed primary glial cultures obtained from neonatal Sprague Dawley rat cortex as described previously (Pompili et al., 2006). Glial cells were seeded onto T75 flasks, and maintained in Advanced Dulbecco's Modified Eagle's Medium (DMEM) supplemented with 10% foetal calf serum (FCS) (Invitrogen, Carlsbad, CA, USA) in 5% CO_2. Astroglial cultures consisted of >95% glial fibrillary acidic protein-positive cells.

Astrocytes (1×10^5 cells/cm^2) were seeded onto 96, 24 or 6-well plates depending on the experiment. After 24 h from seeding cells were treated with TMT (1, 5, 10, 20 mM; Heraeus, Karlsrube, Germany), 0.5 mM staurosporine, lithium chloride (0.5, 1, 2, 10 mM), rapamycin (0.5, 1, 2 mM), 10 mM indirubin-3′-monoxime, 100 nM bafylomicin A1, 50 mM chloroquine, 5 mM 3-methyladenine. All these compounds were used alone or in combination for different times ranging from 3 to 48 h as reported in the figure legends. All reagents were from Sigma–Aldrich unless otherwise stated.

2.2. Assessment of cell death

Cell death was evaluated by measuring the release of lactate dehydrogenase (LDH) in the culture medium by the Cytotoxicity Detection Kit (Roche, Mannheim, Germany) according to manu-facturer's protocols.

The DNA fragmentation of apoptotic cells was detected using the terminal deoxynucleotidyl transferase-mediated biotinylated UTP nick end labelling (TUNEL) kit (In situ Cell Death Detection Kit, Roche). Cells were cultured on coverslips and at the end of the drug treatment fixed in 4% paraformaldehyde in 0.1 M phosphate buffer pH 7.4 (PBS) at room temperature for 15 min and then incubated with a permeabilizing solution (0.1% Triton X-100) for 10 min at 4 8C. The cells were then incubated with the TUNEL reaction mixture for 60 min at 37 8C and visualized by inverted fluorescence microscopy (Eclipse E600, Nikon Instruments SpA, Italy). TUNEL- positive nuclei were counted in 10 nonoverlapping fields per coverslip and then converted to percentage by comparing TUNEL- positive counts with the total cell nuclei visualized by DAPI (4′,6′-diamino-2-phenylindole) counterstaining.

2.3. Electron microscopy

Astrocytes were treated with TMT for 24 h and then processed for electron microscopy. After washing with PBS, samples were fixed in 0.1% glutaraldehyde, 2% paraformaldehyde in PBS for 1.30 h at 4 8C. After washing with PBS, samples were post-fixed in 1% OsO_4 for 1 h at 4 8C and dehydrated in decreased series of ethanol and embedded in Epoxy resin. Ultrathin sections (40–50 nm) of adherent astrocytes on Termanox were cut at ultramicrotome. Sections were contrasted with uranyl acetate (saturated solution in methanol) and lead citrate and examined using a Jeol JEM SX 100 electron microscope (Jeol, Tokyo, Japan).

2.4. Immunocytochemistry

After treatment with TMT for 24 h primary astrocytes were fixed in methanol for 5 min, incubated with 10% donkey serum in PBS for 30 min at room temperature and then incubated with a rabbit anti-LC3B antibody (Sigma, Italy) for 1 h at room tempera- ture. After washings samples were incubated with donkey Dy-light 549-labelled anti-rabbit IgG (1:400; Jackson ImmunoResearch Laboratories) for 30 min at room temperature. The fluorescence was visualized under Nikon fluorescent microscope (Eclipse E600; Nikon Instruments S.p.A., Firenze, Italy). No significant fluorescent signal was detected with the secondary antibody alone.

2.5. Western blotting

Treated and untreated cells were lysed in RIPA buffer contain- ing protease and phosphatase inhibitors (Protease Inhibitor Cocktail and Phosphatase Inhibitor Cocktail 2, Sigma). For estimation of p62 levels only, cells were lysed directly in 100 ml 2× SDS-PAGE gel loading buffer (125 mM Tris–HCl, pH 7.4, 4% SDS, 0.04% bromophenol blue, 30 mg/ml DTT added immediately beforeuse), sonicated 3 times for 5 s and then boiled for 5 min (Bjørkøy et al., 2009). All samples were clarified by centrifugation at 1000 rpm for 5 min. Equivalent amount of protein (10 mg) from each sample was electrophoretically resolved on 12.5% precast SDS-polyacrylamide gels (ExcelGel, GE Healthcare Biosciences) using horizontal apparatus (Pharmacia Biotech, Uppsala, Sweden). Then, separated proteins were electro-transferred onto nitrocellu- lose membranes (Schleicher & Schuell) by a semi-dry system (Novablot, Pharmacia Biotech). Membranes were blocked with 3% non-fat milk (5% BSA for anti-phospho-GSK3) in PBS and then incubated (overnight at 4 8C) with the following antibodies: anti-LC3B (Sigma), anti-p62/SQSTM1 (MBL, PM045), anti-phospho- GSK3a/b (Ser 21/9) (Cell Signalling). After extensive washing with PBS containing 0.1% Tween-20 (TBST), blots were incubated with 1:2000 dilution of HRP-conjugated secondary

antibody (Amersham Biosciences) for 1 h at room temperature. Immunopositive bands were detected with a chemiluminescence detection system (GE Healthcare Biosciences). To check for equal loading of the gel, membranes were stripped and reprobed with mouse anti-b-actin or anti-GAPDH antibodies (1:20,000, Sigma). Densitometric analysis was performed with the Quantity One software (BioRadLaboratories).

2.6. Transfection

Astrocytes were seeded at $2 \times 10^4/cm^2$ onto chamber slides (m-slide 8 well, Ibidi). After 24 h from seeding they were transfected using Lipofectamine 2000 according to the manufac- turer protocol. The vector pBABE-puro-mCherry-EGFP-LC3B was obtained from Addgene. Twenty-four hours after transfection cells were treated with TMT or 0.5 mM lithium (used as positive control) for 3 h, fixed with 4% paraformaldehyde in PBS for 20 min at room temperature, washed and mounted with Vectashield. Images were collected using Leica confocal microscope (Laser Scanning TCS SP2) (Leica Microsystems Wetzlar, Germany).

For time-lapse experiments astrocytes were transfected as previously reported and 24 h after transfection they were treated with TMT. At 3 h of treatment images were recorded for 1–2 h.

All time-lapse images of EGFP-mCherry-LC3B transfected astrocytes were obtained with Leica confocal microscope (Laser Scanning TCS SP2) equipped with Ar/ArKr and HeNe lasers coupled to a dark microscope incubator maintained at 37 8C and 5% CO_2. Laser line was at 488 nm and 543 nm for EGFP and mCherry excitation, respectively. Images were scanned under a 40× oil immersion objective with a cycle time of 2 min, at constant laser intensity with a 1024 × 1024 pixel resolution and were processed using LEICA confocal software. The motility of EGFP and mCherry labelled vesicles was drawn with Leica confocal software.

2.7. Labelling of lysosomes

Astrocytes seeded onto 24-well plates containing glass cover- slips were treated with TMT, 100 nM bafylomicin A1 or 50 mM chloroquin. At 3 and 24 h of treatment 100 nM Lysotracker Red DND 99 (Life Technologies) was added for 30 min at 37 8C in the dark. After washes in PBS, cells were fixed in 4% paraformaldehyde in PBS for 20 min at room temperature. Coverslips were then mounted with Vectashield (H1200 Vector Laboratories) and analyzed under a fluorescence microscope (Eclipse E600, Nikon Instruments SpA, Italy).

2.8. Animals and immunohistochemistry

Male Sprague Dawley rats (7 week-old, weighing 250 g) (Charles River, Italy) were housed in a temperature and humidity-controlled room (21 5 8C and 60% humidity) and fed ad libitum with standard laboratory diet and water. All procedures were carried out in accordance with the Italian laws and guidelines established for the care and the use of animals in research. Rats were administrated a single intraperitoneal dose of TMT (8 mg/kg body weight; Heraeus, Karlsrube, Germany) or vehicle (saline) and were sacrificed at 21 days after treatment. Brains were rapidly removed, embedded in OCT compound (Killik, Bio-Optica, Italy), and frozen on methylbutane precooled with liquid nitrogen as previously reported (Pompili et al., 2011).

Sagittal cryostatic sections (7-mm thickness) from saline and TMT-treated rats were fixed with 4% paraformaldehyde in PBS (pH 7.4) at room temperature for 10 min. After quenching autofluor- escence with 0.05 M ammonium chloride and saturation of nonspecific sites with 3% normal donkey serum (BioCell Research Laboratories, Rancho Dominguez, CA) and 0.1% Triton X-100, sections were incubated overnight at 4 8C with rabbit anti-p62 (1:500; MBL, PM045) and mouse anti-S100b (1:1000; Sigma– Aldrich, clone SH-B1). After washing, the sections were incubated with a mixture of donkey Dy-light 549 anti-rabbit IgG (1:400; Jackson ImmunoResearch Laboratories, West Grove, PA) and donkey Dy-light 488-labelled anti-mouse IgG (1:200; Jackson ImmunoResearch Laboratories). Negative controls were performed substituting specific Igs with an equivalent amount of nonspecific Igs and omitting primary antibodies. Slides were mounted with Vectashield mounting medium, containing DAPI for nuclear staining (Vector Laboratories, Burlingame, CA). Examinations and photographs were made using a fluorescence microscope (Eclipse E600; Nikon Instruments S.p.A., Firenze, Italy).

2.9. Statistics

Statistical analyses were conducted using GraphPad Prism version 4.00 software. Data are expressed as averages SD. Comparisons were analyzed using one-way ANOVA with Bonfer- roni-corrected t test. All experiments were performed in triple and reproduced at least four times.

3. Results

Primary astrocytes were treated with increasing concentrations of TMT and cytotoxicity evaluated by LDH release (Fig. 1A). TMTtoxicity started to be statistically significant at the 10 mM dose which induced a cell loss of 27 2% at 24 h and of 42 5% at 48 h (Fig. 1A). The 10 mM concentration which corresponded to

the minimum TMT dose affecting cell viability was used in all further experiments. The analysis of cell death at earlier time points indicated
that in astroglial cell cultures the number of apoptotic cells started to increase significantly respect to control at 8 h of TMT treatment (12 3%); this number then continued slightly to augment at 24 h (18 4%) (Fig. 1B). TUNEL-positive cells in the untreated control were 3–4% at all times tested while in staurosporine-treated samples (positive control) their number reached 30% at 24 h.

The ultrastructural analysis by transmission electron micros- copy (EM) of the ongoing intoxication of TMT-treated astrocytes revealed that their main morphological feature was an extensive vacuolization of the cytoplasm with some of the accumulating vesicles resembling autophagic vacuoles (AVs) (Fig. 2). In particu- lar, these vesicles appeared to contain flocculated and precipitated material (Fig. 2B) or part of the cytoplasm with various degrees of electrondensities (Fig. 2C). Alteration of the mitochondrial morphology was also detected in TMT-treated astrocytes (Fig. 2B and C) in line with our previous observations in neurons(Fabrizi et al., 2012).

In order to better characterize the numerous vesicles appearing in the EM images of TMT-treated samples, we labelled astrocytes with an anti-LC3 antibody which is considered the most reliable marker for identifying AVs. Consistently with the EM observations, the analysis of LC3 expression confirmed the presence of a great number of AVs in astrocytes following TMT treatment (Fig. 3B andC) while few of these vesicles were detected in the untreated control (Fig. 3A).
It is known that the presence of a great number of AVs in a sample does not necessarily correspond to an increased autophagic flux since it can also be related to an impairment of the maturation of these vesicles. Thus, we decided to check the LC3-I/II conversion by western blot analysis in astrocytes treated with TMT alone or in combination with bafilomycin A1. Being a potent inhibitor of the vacuolar-type H+ ATPase, bafilomycin A1 impairs lysosomal functions blocking late stages of autophagy and consequently LC3 degradation (Yamamoto et al., 1998; Boya et al., 2005). Samples treated with TMT or TMT + bafilomycin A1 for 3 h showed

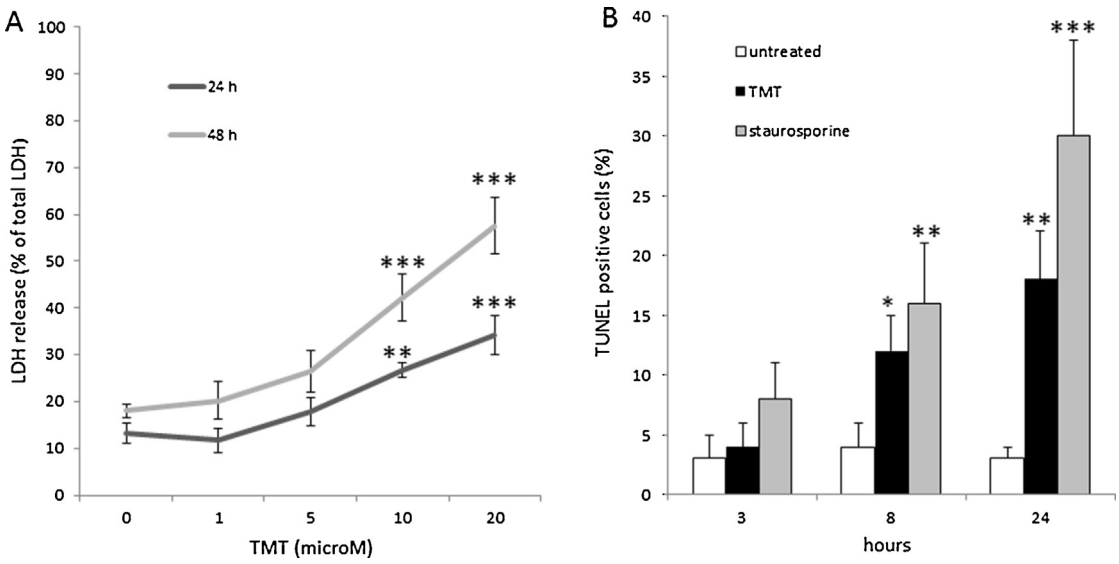

Fig. 1. Cytotoxic effect of TMT in astrocyte primary cultures. (A) LDH release in the culture medium of astrocytes treated with increasing concentrations of TMT (1, 5, 10, 20 mM) for 24 and 48 h. The lowest dose of TMT significantly affecting cell viability is 10 mM. (B) Apoptotic cells labelled by TUNEL appeared at 8 h after 10 mM TMT treatment and their number slightly increased further at 24 h. The percentage of apoptotic nuclei detected after 0.5 mM staurosporine treatment is shown as reference. Averages SD of four independent experiments. ANOVA with Bonferroni's corrected *t* test. $*p \leq 0.05$, $**p \leq 0.01$, $***p \leq 0.001$ versus untreated control.

similar LC3-II levels (Fig. 4A and B) indicating that late stages of autophagy were already blocked by TMT alone. The observed impairment in autophagy induced by TMT persisted up to 48 h (not shown). A further confirmation of a block in AVs maturation after TMT came from experiments performed using astrocytes tran- siently transfected with LC3 expressed in tandem with two fluorochromes EGFP (which is lost in acidic compartments) and mCherry (which conversely is stable in acidic compartments). This method enables the simultaneous analysis of autophagosomes (EGFP+/mCherry+) and autophagolysosomes (EGFP—/mCherry+). In agreement with western blot analyses, TMT treatment

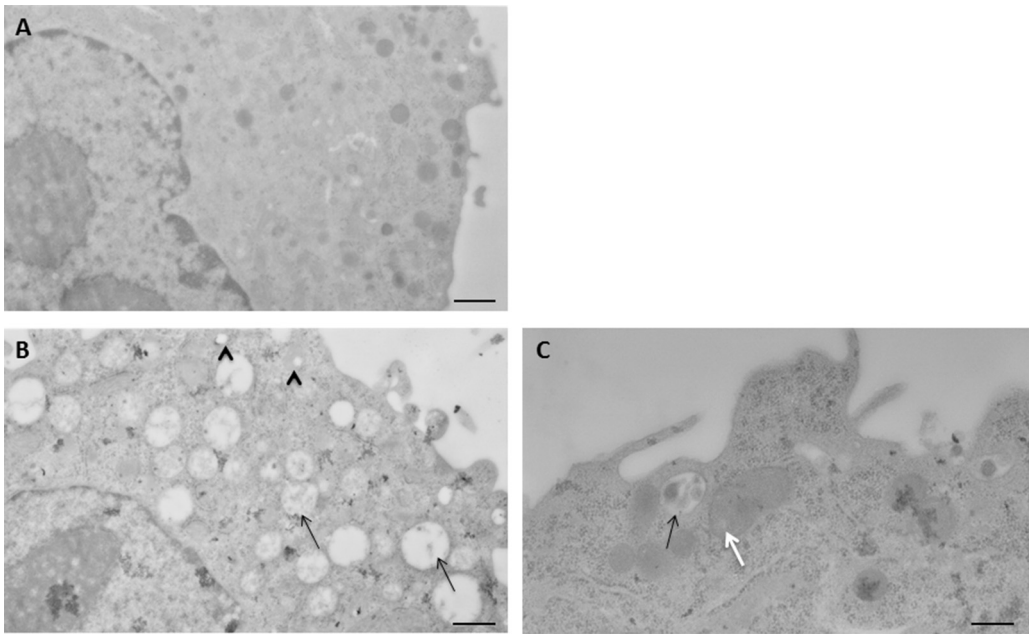

Fig. 2. Ultrastructural analysis of astrocytes treated with TMT. Electron microscopic images of astrocytes left untreated (A) or treated with TMT for 24 h (B, C). An extensive vacuolization of the cytoplasm is induced in astrocytes by TMT. Some of these vacuoles resembles autophagic vesicles (black arrows) containing precipitated material (B, C). An autophagic-like vesicle with cytoplasmic material is visible at higher magnification in (C). Altered mitochondria with matrix dilution are shown in (B) (arrowheads) and in (C) (white arrow). Scale bar 1.05 mm (A), 1.09 mm (B), 0.56 mm (C).

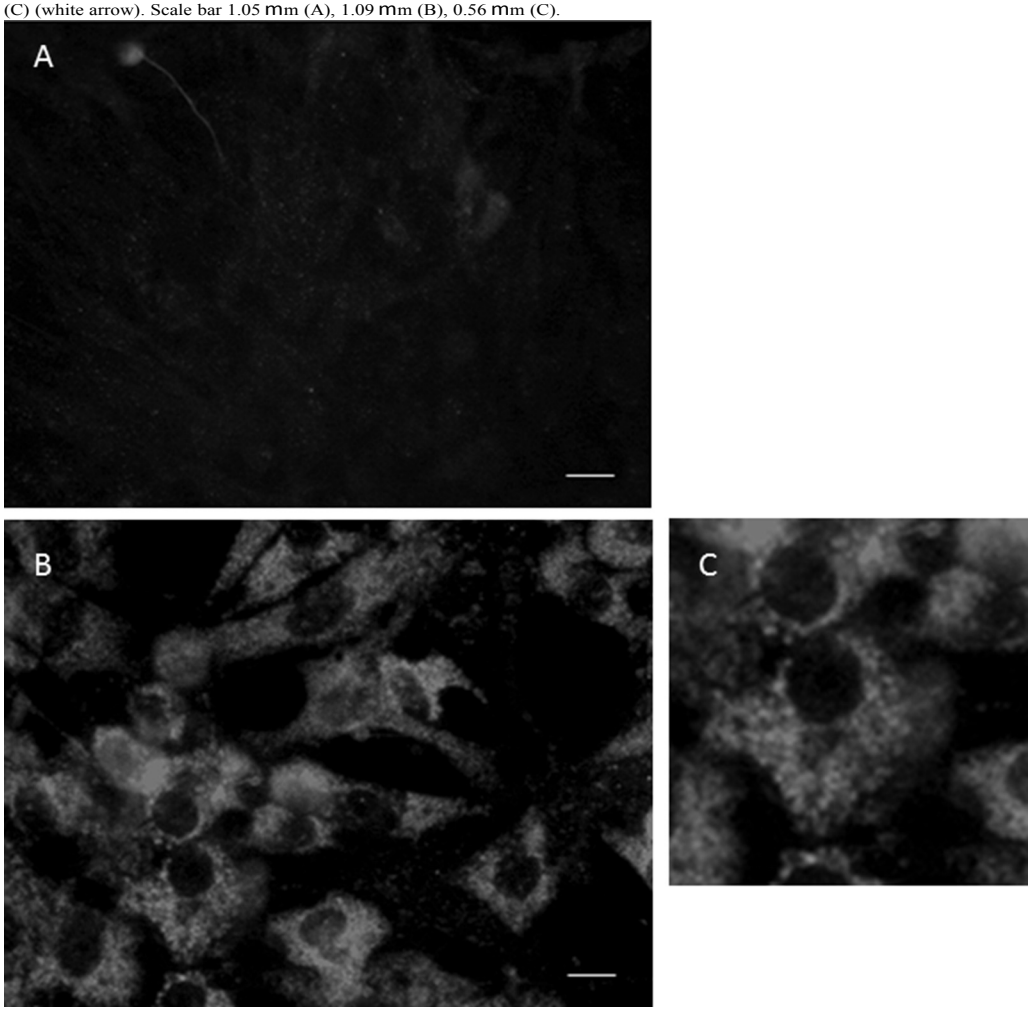

Fig. 3. LC3 expression in astrocytes following TMT treatment. Numerous autophagic vesicles labelled with LC3 are detected after 24 h of TMT treatment in astrocytes (B) whilea faint staining is observed in the untreated control cells (A). In (C) an enlargement of (B) is shown in order to allow a better visualization of vesicles. Scale bar = 5 mm.

brain of TMT-intoxicated rats were also highly labelled with an anti-p62 antibody (Fig. 6B). Astrocytes were identified by the pan- astrocytic marker S100b (Raponi et al., 2007).

Since TMT appeared to block the late stages of autophagy, we decided to control the status of lysosomes by Lysotracker Red staining. This compound is known to selectively accumulate in cellular compartments with low internal pH. As shown in Fig. 7, a similar Lysotracker Red staining was obtained in astrocytes treated with TMT for 3 h and in the correspondent untreated control. Conversely, treatments with bafylomicin A1 and chloroquine which are known to raise lysosomal pH resulted in a very faint Lysotracker Red signal (Fig. 7). Lysosomes appeared still similar to controls at 24 h of TMT treatment (not shown). When we checked the status of microfilaments and microtubules in TMT-treated astrocytes we did not detect any gross modification in the cytoskeletal architecture at 3 h of TMT treatment (not shown).

Thus, in order to track and follow the fate of AVs, we performed time-lapse recordings of EGFP-mCherry-LC3B transfected astro- cytes. Data were collected after 3 h of TMT treatment, a time point which corresponded to a complete impairment of autophagy as shown by previous data. The main difference observed between the TMT-treated and the control samples was that while in untreated cells the few autophagosomes present rapidly travelled towards the perinuclear area evolving into autophagolysosomes, inTMT-treated astrocytes the numerous autophagosomes detected never formed autophagolysosomes maintaining mainly the same position during our 1 h observation (Fig. 8). We recorded images even for 2 h obtaining the same result although the fluorescent signal became gradually fainter (not shown).

It has been recently reported that lithium can limit TMT neurotoxicity in intoxicated rodents (Kim et al., 2013; Yoneyama et al., 2014), but its mechanism of action remains elusive for its multiple molecular targets (Pasquali et al., 2009). When lithium was used in combination with TMT in our astrocyte cultures, this cation did not modify the TMT-induced increase in LC3-II and p62 (Fig. 9A). That is lithium was unable to overcome the autophagic block imposed by TMT. Similar data were obtained with another known inducer of autophagy such as rapamycin (not shown). Conversely, when we used an inhibitor of autophagy such as 3- methyladenine (3-MA; blocker of the sequestration stage) (Stroikin et al., 2004), a cell loss 30 2% was observed in astrocyte cultures as measured by LDH release at 24 h; the combination of 3- MA and TMT raised cytotoxicity to 38 3% (not shown).

Interestingly, although unable to modify the autophagic block caused by TMT, lithium could still rescue astrocytes from TMT toxicity (Fig. 9B). This effect correlated well with the ability of this cation of increasing the phosphorylation/inactivation of glycogen kinase synthase-3b (GSK-3b) (Fig. 10A). A similar protective effect was also observed using another known GSK-3 inhibitor such as indirubin-3^{0} monoxime (Fig. 10B

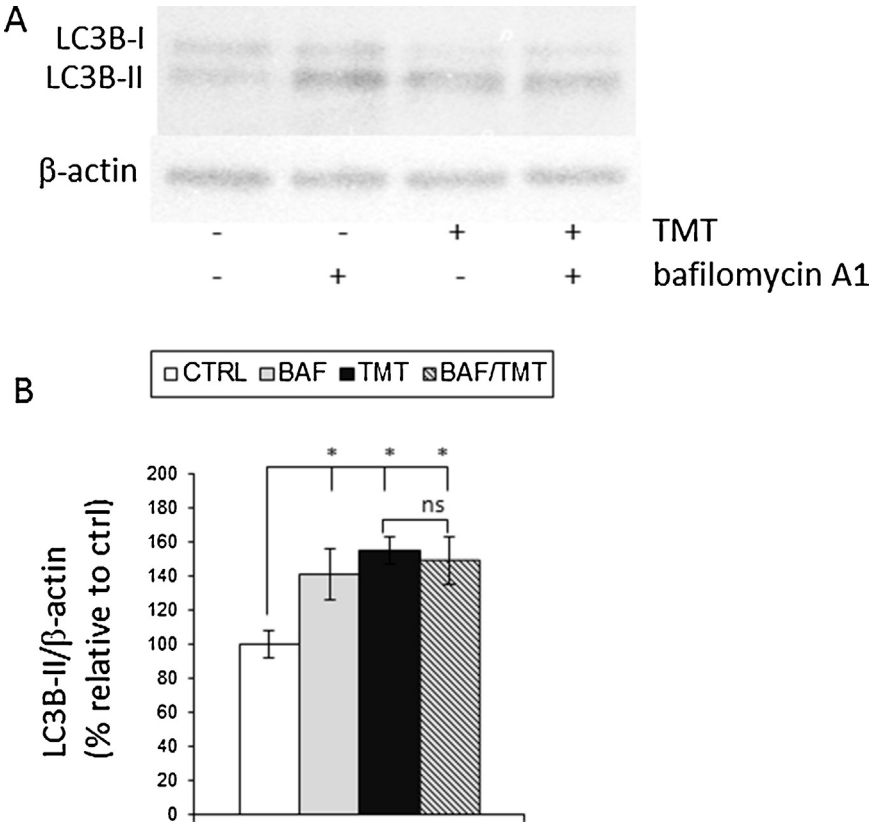

Fig. 4. LC3 turnover assay in TMT-treated astrocytes in the presence of a lysosomal inhibitor. (A) Western blot analysis of LC3-I/II conversion in astrocytes treated for 3 h with TMT alone or in combination with 100 mM bafilomycin A1; (B) densitometric analysis of Western blot data shown in (A). Averages SD of four independent experiments. ANOVA with Bonferroni's corrected *t* test. *$p \leq 0.01$ versus untreated control; ns, not significant, TMT versus TMT + bafilomycin A1 (BAF/TMT).

4. Discussion

Autophagic vacuoles (AVs) have been detected by ultrastruc- tural studies in the brain of TMT-treated rodents (Bouldin et al., 1981) and the presence of similar vesicles was reported to occur in the affected areas of intoxicated human brains (Besser et al., 1987). Cytoplasmic vacuolization is observed in vitro after exposure to a variety of chemicals and generally protect cells by the isolation and buffering of toxins (Aki et al., 2012). Although autophagy is primarily considered to have a cytoprotective function, it can also promote cell death through a sort of self-cannibalism (Nikoletopoulou et al., 2013).

Here we show that in astrocyte cultures a great number of AVs appeared few hours after TMT administration. However, when we analyzed more in detail the autophagic flux in TMT-treated astrocytes, we observed that the accumulation of autophago- somes was not due to an increase in the autophagic flux but to an impairment of the late stages of autophagy. The occurrence of this block was demonstrated by the western blot analysis of the LC3-I/ II conversion after TMT in combination with an inhibitor of lysosomal acidification (bafylomicin A1). It was then confirmed by the confocal analysis of AVs in mCherry-EGFP-LC3B trans- fected astrocytes which allows the visualization of both autophagosomes and autophagolysosomes. The average half-life for AVs has been reported to be about 10 min (Pfeifer, 1978; Schworer et al., 1981; Mizushima et al., 2001) and in line with those previous data, in our culture system autophagosomes rapidly evolved into autophagolysosomes in untreated astro- cytes. The time-lapse recordings of these vesicles showed their movement mainly towards the perinuclear area. Conversely, in TMT-treated astrocytes autophagosomes remained almost immobile during our 1 h observation and even longer without evolving into autophagolysosomes.

Autophagosome dynamics rely on their interaction with the cytoskeleton and especially with the microtubules (MTs) (Mon- astyrska et al., 2009). A trafficking of autophagosomes along MTs towards lysosomes is necessary to allow their effective fusion (Kimura et al., 2008) and the disruption of microtubule structure inhibits autophagosome trafficking and maturation (Aplin et al., 1992; Webb et al., 2004). It is possible that the observed impairment in AVs movement is related to the reported ability of TMT to inhibit microtubule assembly (Jensen et al., 1991). To note this impairment in autophagy was detected already at 3 h of TMT treatment when no gross morphological changes were observed neither at the level of the cytoskeleton nor in the lysosomal compartment. Besides, the observed block in autophagy preceded of several hours the occurrence of cell death. In fact, apoptotic cells started to increase their number significantly respect to control at 8 h of TMT treatment.

Consistently with an impairment of autophagy we observed in TMT-treated astrocytes the accumulation of p62, a protein which is specifically degraded through this pathway. Interestingly, when we checked the expression of p62 in the brain of rats intoxicated with TMT high levels of this protein were also detected in the reactive astrocytes present in the hippocampus, a brain area highly damaged by this toxic compound as mentioned before (Chang and Dyer, 1985; Kawada et al., 2008). To note the inhibition of the autophagic flux and the p62-dependent activation of the kep1- Nrf2 pathway has been reported to occur following the exposure to other toxic molecules, such as arsenic (Lau et al., 2013). Besides, the Nrf2/p62 signalling pathway is involved in the apoptosis resistance from cadmium exposure (Son et al., 2014

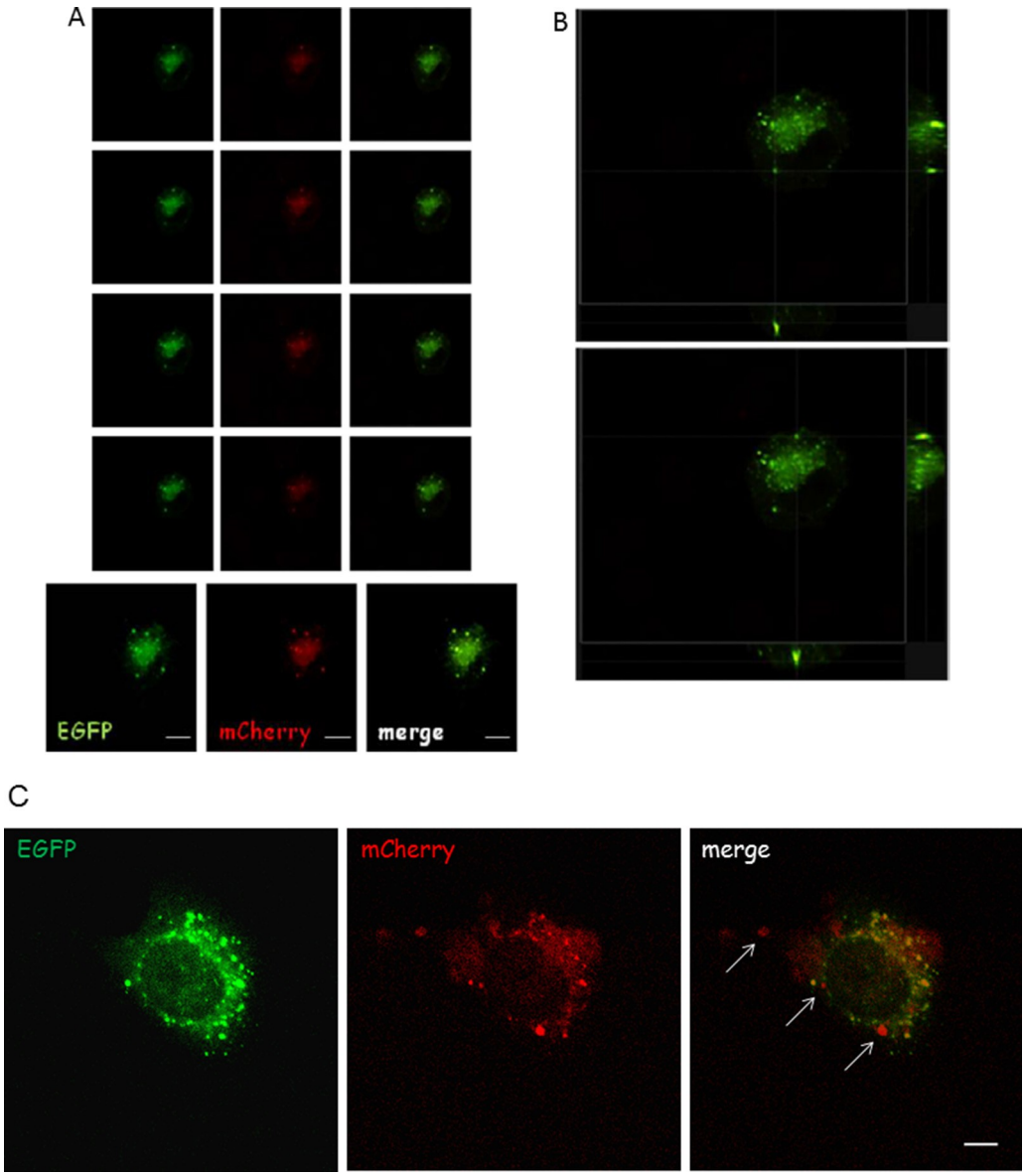

Fig. 5. Confocal analyses of autophagic vesicles in mCherry-EGFP-LC3-transfected astrocytes. (A) After 3 h of TMT treatment many autophagosomes (EGFP+/mCherry+) but no autophagolysosomes (EGFP—/mCherry+) are observed. A representative part of one spatial series composed of 23 optical sections with a step size of 0.5 mm of TMT treated cell is shown. The images were scanned under a 40× objective with a 3× electronic zoom. The correspondent maximum projection of the series is shown at the bottom. Scale bar = 20 mm. (B) Colocalization analysis of the series showing a perfect overlapping of the two fluorochromes. (C) Lithium (0.5 mM; inducer of autophagy) determines in astrocytes the appearance of both autophagosomes (EGFP+/mCherry+) and autophagolysosomes (EGFP—/mCherry+). White arrows, drawn in the right panel (merge), indicate specifically autophagolysosomes. Maximum projection of a spatial series composed of 7 optical sections with a step size of 1 mm is shown. Scale bar = 5 mm.

Lithium has been reported to rescue seizures and to ameliorate memory deficits in TMT-intoxicated rodents increasing at the same time the inhibitory phosphorylation of GSK-3 in the hippocampus (Kim et al., 2013). Moreover, lithium enhances neuritogenesis ameliorating the depression-like behaviour observed in mice treated with TMT (Yoneyama et al., 2014). To note, a potential role of autophagy in depression has been recently reported (Gassen et al., 2014). Lithium mechanism of action is difficult to assess for its multiple molecular targets. In fact, it can increase the autophagic flux by inhibiting IMPase while it can inhibit autophagy acting through GSK-3 (Sarkar et al., 2008). Also lithium upregulates the expression of neurotrophins and growth factors while con- cominantly it downregulates pro-apoptotic factors displaying its neuroprotective activity in a variety of neurological and neurodegenerative disorders (for a recent review see Leedset al., 2014).

Our results are in line with the above-mentioned published data (Kim et al., 2013; Yoneyama et al., 2014). In fact, in our astrocyte cultures lithium limited TMT toxicity. To note this effect can be obtained at relatively high concentrations (2 mM) and is
accompanied by the phosphorylation of GSK-3b. When we used
rapamycin or low doses of lithium in order to promote autophagy in astrocytes no rescue from TMT toxicity was observed. As appeared from the western blot analyses of LC3-I/II and of p62, the block of autophagy imposed by TMT cannot be forced by lithium atnone of the concentrations tested (0.5–2 mM). Thus, this cation
appeared to exert its pro-survival action through a pathway different from autophagy possibly acting at the GSK-3b level. Inline with this hypothesis, a significant reduction in TMT toxicity

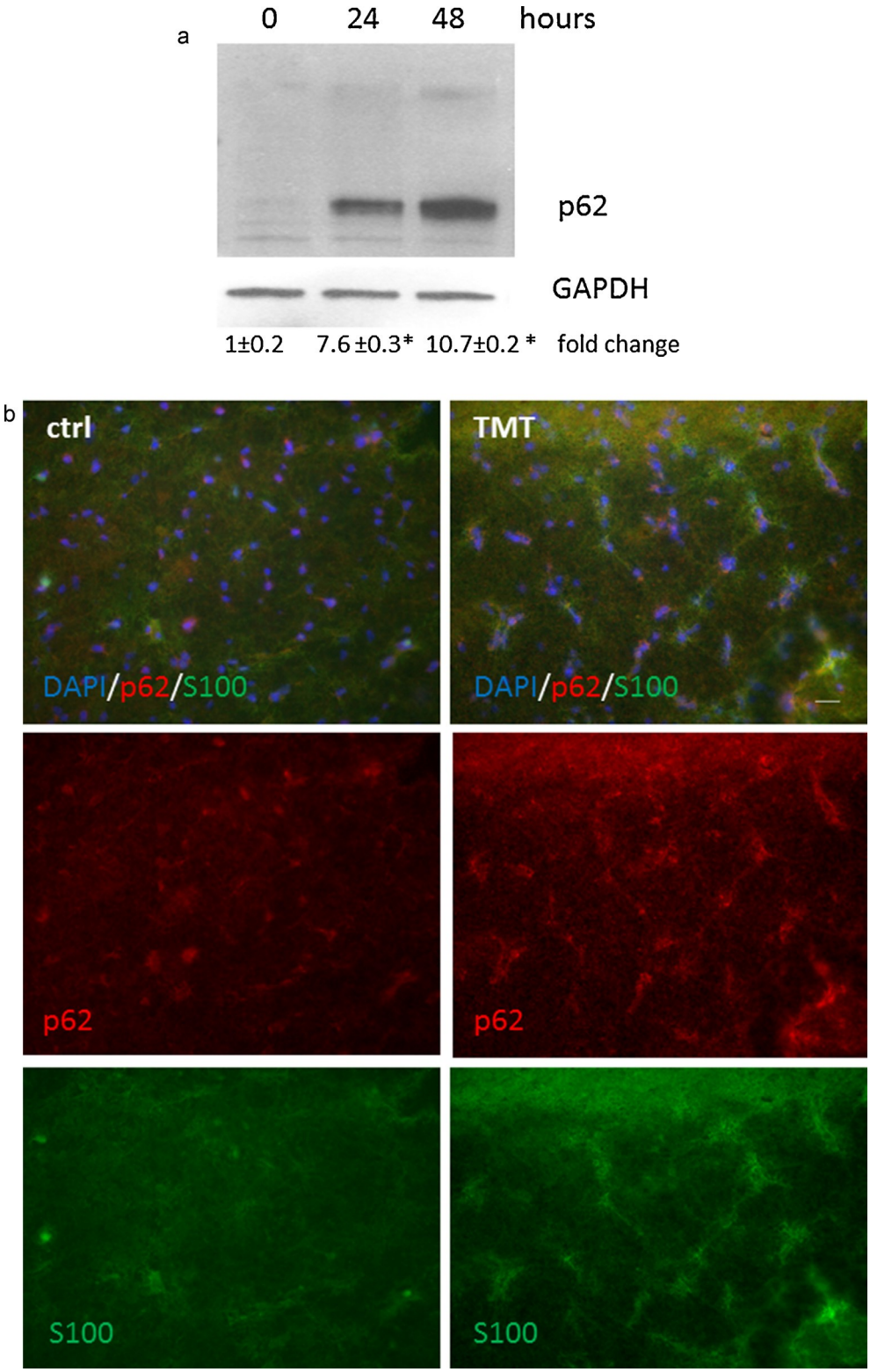

Fig. 6. Accumulation of p62 following TMT treatment. (A) Western blot analysis of p62 expression in astrocyte cultures treated for 24 and 48 h with TMT. The level of GAPDH is shown as reference. *$p \leq 0.01$ versus untreated control. (B) Immunofluorescence analysis of p62 and S100b in the CA3/hilus hippocampal subfields from control and TMT-treated rats sacrificed 21 days after TMT intoxication. Nuclei are counterstained with DAPI. Scale bar = 10 mm.

was also observed with a known inhibitor of GSK-3b such as indirubin-3′ monoxime. Besides, GSK-3 and particularly the GSK-3b isoform has been identified as having a proapoptotic effect in many settings (Li et al., 2002).

In conclusion, our results show that in astrocytes TMT completely blocks the autophagic flux after few hours of treatment and this impairment of autophagy imposed by TMT cannot be overcome by known autophagy inducers such as lithium or rapamycin. A rescue from TMT toxicity can nevertheless be obtained by using concentrations of lithium which determine the phosphorylation/inactivation of

GSK-3b

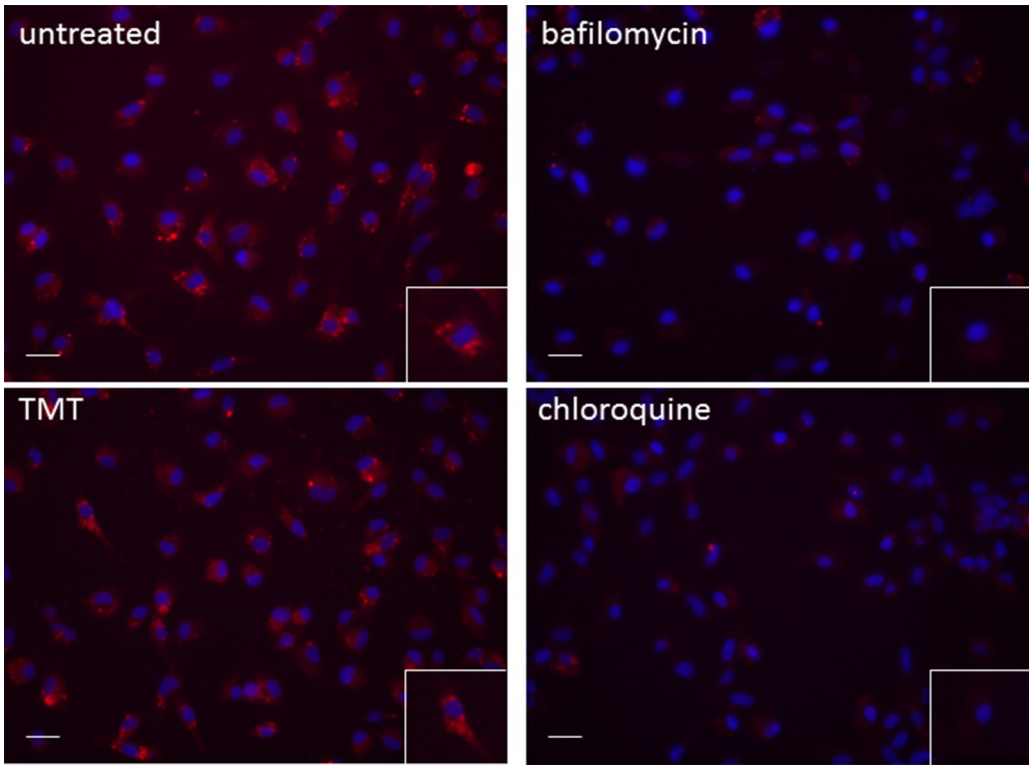

Fig. 7. Lysosome labelling by Lysotracker Red in astrocytes exposed to TMT or lysosomal inhibitors. After treatment for 3 h with TMT, chloroquine (50 mM) or bafylomicin A1 (100 nM) astrocytes were stained with Lysotracker Red. The lysosomotropic agents chloroquine and bafylomicin A1 were used as controls since they are known to affect lysosome acidification. An enlargement of a single cell for each treatment is shown on the right. Nuclei were counterstained with DAPI. Scale bar = 10 mm.

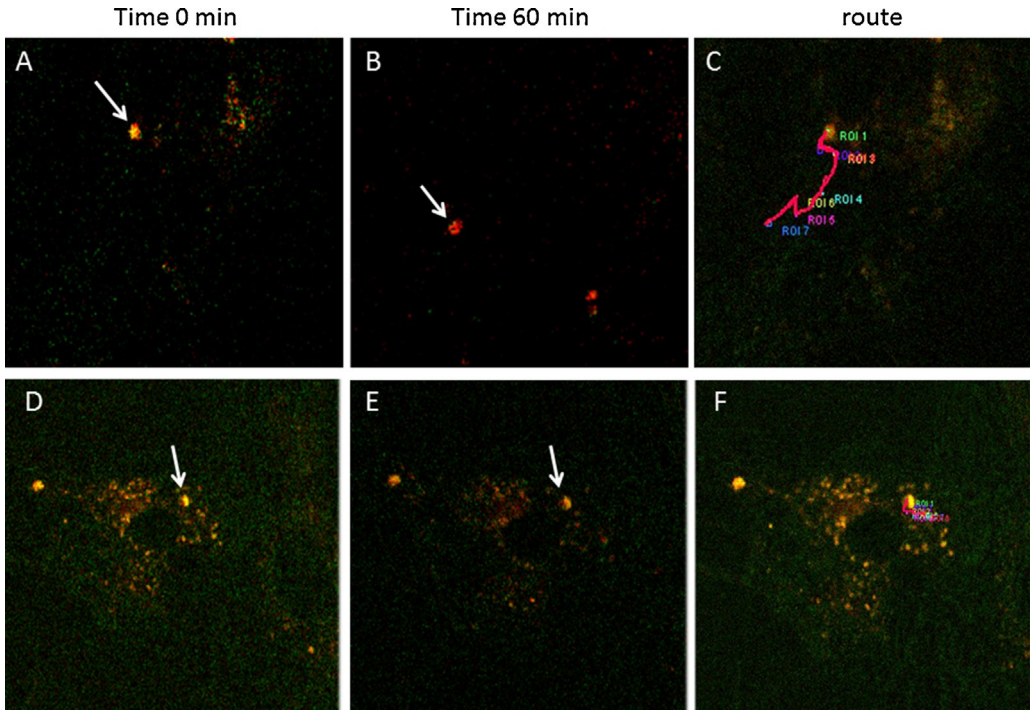

Fig. 8. Movement of autophagic vesicles (AVs) is impaired after TMT. Representative time-lapse images at time 0 (A, D) and 60 min (B, E) of AVs in control (A, B) and in TMT treated (D, E) EGFP-mCherry-LC3B transfected astrocytes. In C and F the route performed by a representative autophagosome in control (C) and TMT treated cells (F) is reported. All images represent the merging pictures of EGFP signal (green) and mCherry signal (red). The presence of a red only signal indicates the fusion of the autophagosome with a lysosome to form an autophagolysosome (B). It is well evident that in TMT treated astrocytes, the AV movement (red line in F) was reduced respect to control (red line in C). (For interpretation of the references to colour in this legend, the reader is referred to the web version of the article.)

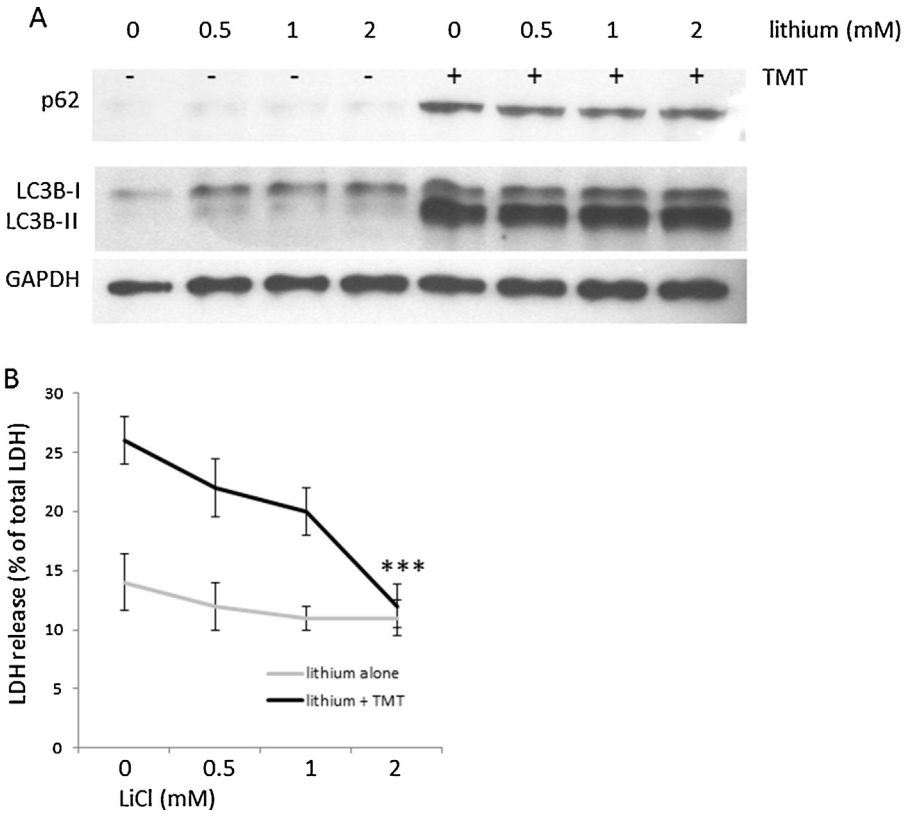

Fig. 9. Lithium protects astrocytes from TMT toxicity without affecting the TMT-induced autophagic block. (A) Western blot analysis of LC3 and p62 expression in astrocytes treated for 24 h with TMT alone or in combination with lithium (0.5, 1 and 2 mM). GAPDH is shown as loading reference control. (B) Astrocytes were treated with TMT alone or in combination with different doses of lithium (0.5, 1, 2 mM) and cytotoxicity assessed at 24 h measuring LDH release. Averages SD of four independent experiments. ANOVAwith Bonferroni's corrected *t* test. ***$p \leq 0.001$ versus untreated control.

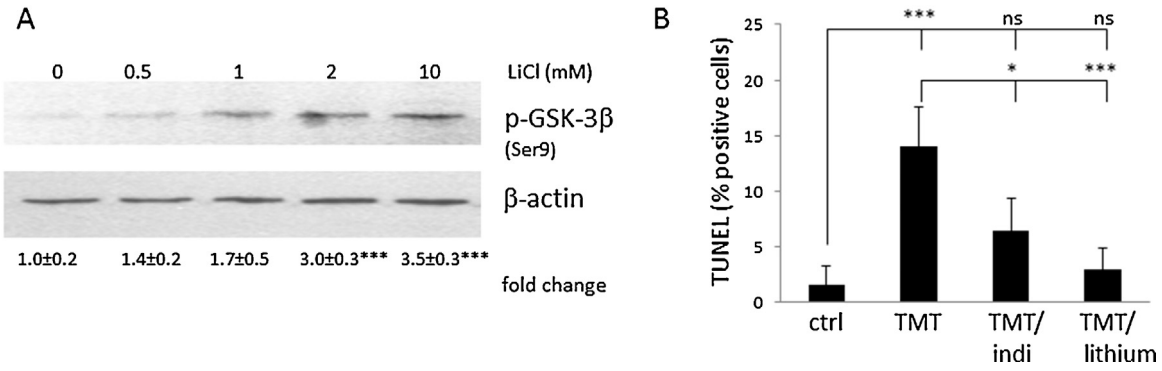

Fig. 10. Lithium rescues astrocytes from TMT-induced cell death at doses which determines the phosphorylation/inactivation of GSK-3b. (A) GSK-3b phosphorylation in astrocytes treated with doses of lithium ranging from 0.5 to 10 mM for 24 h was observed by Western blot. The level of expression of b-actin is shown as reference. Densitometric analysis of the bands shows a significant increase in GSK-3 phosphorylation respect to control at the 2 mM dose and above. Averages SD of four independent experiments. ANOVA with Bonferroni's corrected *t* test. ***$p \leq 0.001$ versus untreated control. (B) Lithium (2 mM) and indirubin-3^{0}-monoxime (indi; 10 mM) reduce the number of apoptotic cells in astrocyte cultures treated with TMT for 24 h. Averages SD of four independent experiments. ANOVA with Bonferroni's corrected *t* test. *$p \leq 0.05$, ***$p \leq 0.001$ versus untreated control or TMT alone as indicated.

Conflict of interest

None declared.

Acknowledgements

These studies were supported by grants awarded by Universita`Sapienza (Ricerche Universitarie) to LF.

References

Aki, T., Nara, A., Uemura, K., 2012. Cytoplasmic vacuolization during exposure todrugs and other substances. Cell Biol. Toxicol. 28 (3), 125–131.

Aldridge, W.N., Street, B.W., Skilleter, D.N., 1977. Oxidative phosphorylation, halide-dependent and halide-independent effects of triorganotin and trioganolead compounds on mitochondrial functions. Biochem. J. 168 (3), 353–364.

Aplin, A., Jasionowski, T., Tuttle, D.L., Lenk, S.E., Dunn Jr., W.A., 1992. Cytoskeletal elements are required for the formation and maturation ofautophagic vacuoles. J. Cell. Physiol. 152, 458–466.

Besser, R., Krämer, G., Thümler, R., Bohl, J., Gutmann, L., Hopf, H.C., 1987. Acute trimethyltin limbic-cerebellar syndrome. Neurology 37 (6), 945–950.

Bjørkøy, G., Lamark, T., Brech, A., Outzen, H., Perander, M., Overvatn, A., Stenmark, H., Johansen, T., 2005. p62/SQSTM1 forms protein aggregates degraded by autophagy and has a protective effect on huntingtin-inducedcell death. J. Cell Biol. 171 (4), 603–614.

Bjørkøy, G., Lamark, T., Pankiv, S., Øvervatn, A., Brech, A., Johansen, T., 2009. Monitoring autophagic degradation of p62/SQSTM1. Methods Enzymol. 452,181–197.

Boya, P., Gonzalez-Polo, R.A., Casares, N., Perfettini, J.L., Dessen, P., Larochette, N.,Metivier, D., Meley, D., Souquere, S., Yoshimori, T., et al., 2005. Inhibition of macroautophagy triggers apoptosis. Mol. Cell. Biol. 25, 1025–1040.

Bouldin, T.W., Goines, N.D., Bagnell, R.C., Krigman, M.R., 1981. Pathogenesis oftrimethyltin neuronal toxicity. Ultrastructural and cytochemical observations. Am. J. Pathol. 104 (3), 237–249.

Cabezas, R., Avila, M., Gonzalez, J., El-Bachá, R.S., Báez, E., García-Segura, L.M., Jurado Coronel, J.C., Capani, F., Cardona-Gomez, G.P., Barreto, G.E., 2014. Astrocytic modulation of blood brain barrier: perspectives on Parkinson'sdisease. Front. Cell. Neurosci. 8, 211.

Cao, D., Jiang, G., Zhou, Q., Yang, R., 2009. Organotin pollution in China: an overview of the current state and potential health risk. J. Environ. Manag. 90 (Suppl. 1), S16–S24.

Chang, L.W., Dyer, R.S., 1985. Septotemporal gradients of trimethyltin-inducedhippocampal lesions. Neurobehav. Toxicol. Teratol. 7 (1), 43–49.

Ceccariglia, S., D'altocolle, A., Del Fa', A., Silvestrini, A., Barba, M., Pizzolante, F., Repele, A., Michetti, F., Gangitano, C., 2014. Increased expression of Aquaporin 4 in the rat hippocampus and cortex during trimethyltin-inducedneurodegeneration. Neuroscience 274, 273–288.

Davidson, C.E., Reese, B.E., Billingsley, M.L., Yun, J.K., 2004. Stannin, a proteinthat localizes to the mitochondria and sensitizes NIH-3T3 cells to trimethyltin and dimethyltin toxicity. Mol. Pharmacol. 66 (4), 855–863.

Fabrizi, C., Somma, F., Pompili, E., Biagioni, F., Lenzi, P., Fornai, F., Fumagalli, L., 2012. Role of autophagy inhibitors and inducers in modulating the toxicity of trimethyltin in neuronal cell cultures. J. Neural Transm. 119 (11), 1295–1305.

Fent, K., 1996. Ecotoxicology of organotin compounds. Crit. Rev. Toxicol. 26 (1),1–117.

Gassen, N.C., Hartmann, J., Zschocke, J., Stepan, J., Hafner, K., Zellner, A., Kirmeier, T., Kollmannsberger, L., Wagner, K.V., Dedic, N., Balsevich, G., Deussing, J.M., Kloiber, S., Lucae, S., Holsboer, F., Eder, M., Uhr, M., Ising, M.,Schmidt, M.V., Rein, T., 2014. Association of FKBP51 with priming of autophagy pathways and mediation of antidepressant treatment response: evidence in cells, mice, and humans. PLoS Med. 11 (11), e1001755.

Haga, S., Haga, C., Aizawa, T., Ikeda, K., 2002. Neuronal degeneration and glialcell-responses following trimethyltin intoxication in the rat. Acta Neuropathol. 103 (6), 575–582.

Jensen, K.G., Onfelt, A., Wallin, M., Lidums, V., Andersen, O., 1991. Effects of organotin compounds on mitosis, spindle structure, toxicity and in vitro microtubule assembly. Mutagenesis 6 (5), 409–416.

Kabeya, Y., Mizushima, N., Ueno, T., Yamamoto, A., Kirisako, T., Noda, T., Kominami, E., Ohsumi, Y., Yoshimori, T., 2000. LC3, a mammalian homologueof yeast Apg8p, is localized in autophagosome membranes after processing. EMBO J. 19 (21), 5720–5728.

Kawada, K., Yoneyama, M., Nagashima, R., Ogita, K., 2008. In vivo acute treatment with trimethyltin chloride causes neuronal degeneration in the murine olfactory bulb and anterior olfactory nucleus by different cascades ineach region. J. Neurosci. Res. 86 (7), 1635–1646.

Kim, J., Yang, M., Kim, S.H., Kim, J.C., Wang, H., Shin, T., Moon, C., 2013. Possiblerole of the glycogen synthase kinase-3 signaling pathway in trimethyltin-induced hippocampal neurodegeneration in mice. PLoS ONE 8 (8), e70356.

Kimura, S., Noda, T., Yoshimori, T., 2008. Dynein-dependent movement of autophagosomes mediates efficient encounters with lysosomes. Cell Struct. Funct. 33 (1), 109–122.

Lau, A., Zheng, Y., Tao, S., Wang, H., Whitman, S.A., White, E., Zhang, D.D., 2013. Arsenic inhibits autophagic flux, activating the Nrf2-Keap1 pathway in ap62-dependent manner. Mol. Cell. Biol. 33 (12), 2436–2446.

Leeds, P.R., Yu, F., Wang, Z., Chiu, C.T., Zhang, Y., Leng, Y., Linares, G.R., Chuang,D.M., 2014. A new avenue for lithium: intervention in traumatic brain injury. ACS Chem. Neurosci. 5 (6), 422–433.

Levine, B., Kroemer, G., 2008. Autophagy in the pathogenesis of disease. Cell 132(1), 27–42.

Besser, R., Krämer, G., Thümler, R., Bohl, J., Gutmann, L., Hopf, H.C., 1987. Acute trimethyltin limbic-cerebellar syndrome. Neurology 37 (6), 945–950.

Bjørkøy, G., Lamark, T., Brech, A., Outzen, H., Perander, M., Overvatn, A., Stenmark, H., Johansen, T., 2005. p62/SQSTM1 forms protein aggregates degraded by autophagy and has a protective effect on huntingtin-inducedcell death. J. Cell Biol. 171 (4), 603–614.

Bjørkøy, G., Lamark, T., Pankiv, S., Øvervatn, A., Brech, A., Johansen, T., 2009. Monitoring autophagic degradation of p62/SQSTM1. Methods Enzymol. 452,181–197.

Boya, P., Gonzalez-Polo, R.A., Casares, N., Perfettini, J.L., Dessen, P., Larochette, N.,Metivier, D., Meley, D., Souquere, S., Yoshimori, T., et al., 2005. Inhibition of macroautophagy triggers apoptosis. Mol. Cell. Biol. 25, 1025–1040.

Bouldin, T.W., Goines, N.D., Bagnell, R.C., Krigman, M.R., 1981. Pathogenesis oftrimethyltin neuronal toxicity. Ultrastructural and cytochemical observations. Am. J. Pathol. 104 (3), 237–249.

Cabezas, R., Avila, M., Gonzalez, J., El-Bachá, R.S., Báez, E., García-Segura, L.M., Jurado Coronel, J.C., Capani, F., Cardona-Gomez, G.P., Barreto, G.E., 2014. Astrocytic modulation of blood brain barrier: perspectives on Parkinson'sdisease. Front. Cell. Neurosci. 8, 211.

Cao, D., Jiang, G., Zhou, Q., Yang, R., 2009. Organotin pollution in China: an overview of the current state and potential health risk. J. Environ. Manag. 90 (Suppl. 1), S16–S24.

Chang, L.W., Dyer, R.S., 1985. Septotemporal gradients of trimethyltin-inducedhippocampal lesions. Neurobehav. Toxicol. Teratol. 7 (1), 43–49.

Ceccariglia, S., D'altocolle, A., Del Fa', A., Silvestrini, A., Barba, M., Pizzolante, F., Repele, A., Michetti, F., Gangitano, C., 2014. Increased expression of Aquaporin 4 in the rat hippocampus and cortex during trimethyltin-inducedneurodegeneration. Neuroscience 274, 273–288.

Davidson, C.E., Reese, B.E., Billingsley, M.L., Yun, J.K., 2004. Stannin, a proteinthat localizes to the mitochondria and sensitizes NIH-3T3 cells to trimethyltin and dimethyltin toxicity. Mol. Pharmacol. 66 (4), 855–863.

Fabrizi, C., Somma, F., Pompili, E., Biagioni, F., Lenzi, P., Fornai, F., Fumagalli, L., 2012. Role of autophagy inhibitors and inducers in modulating the toxicity of trimethyltin in neuronal cell cultures. J. Neural Transm. 119 (11), 1295–1305.

Fent, K., 1996. Ecotoxicology of organotin compounds. Crit. Rev. Toxicol. 26 (1),1–117.

Gassen, N.C., Hartmann, J., Zschocke, J., Stepan, J., Hafner, K., Zellner, A., Kirmeier, T., Kollmannsberger, L., Wagner, K.V., Dedic, N., Balsevich, G., Deussing, J.M., Kloiber, S., Lucae, S., Holsboer, F., Eder, M., Uhr, M., Ising, M.,Schmidt, M.V., Rein, T., 2014. Association of FKBP51 with priming of autophagy pathways and mediation of antidepressant treatment response: evidence in cells, mice, and humans. PLoS Med. 11 (11), e1001755.

Haga, S., Haga, C., Aizawa, T., Ikeda, K., 2002. Neuronal degeneration and glialcell-responses following trimethyltin intoxication in the rat. Acta Neuropathol. 103 (6), 575–582.

Jensen, K.G., Onfelt, A., Wallin, M., Lidums, V., Andersen, O., 1991. Effects of organotin compounds on mitosis, spindle structure, toxicity and in vitro microtubule assembly. Mutagenesis 6 (5), 409–416.

Kabeya, Y., Mizushima, N., Ueno, T., Yamamoto, A., Kirisako, T., Noda, T., Kominami, E., Ohsumi, Y., Yoshimori, T., 2000. LC3, a mammalian homologueof yeast Apg8p, is localized in autophagosome membranes after processing. EMBO J. 19 (21), 5720–5728.

Kawada, K., Yoneyama, M., Nagashima, R., Ogita, K., 2008. In vivo acute treatment with trimethyltin chloride causes neuronal degeneration in the murine olfactory bulb and anterior olfactory nucleus by different cascades ineach region. J. Neurosci. Res. 86 (7), 1635–1646.

Kim, J., Yang, M., Kim, S.H., Kim, J.C., Wang, H., Shin, T., Moon, C., 2013. Possiblerole of the glycogen synthase kinase-3 signaling pathway in trimethyltin-induced hippocampal neurodegeneration in mice. PLoS ONE 8 (8), e70356.

Kimura, S., Noda, T., Yoshimori, T., 2008. Dynein-dependent movement of autophagosomes mediates efficient encounters with lysosomes. Cell Struct. Funct. 33 (1), 109–122.

Lau, A., Zheng, Y., Tao, S., Wang, H., Whitman, S.A., White, E., Zhang, D.D., 2013. Arsenic inhibits autophagic flux, activating the Nrf2-Keap1 pathway in ap62-dependent manner. Mol. Cell. Biol. 33 (12), 2436–2446.

Leeds, P.R., Yu, F., Wang, Z., Chiu, C.T., Zhang, Y., Leng, Y., Linares, G.R., Chuang,D.M., 2014. A new avenue for lithium: intervention in traumatic brain

injury. ACS Chem. Neurosci. 5 (6), 422–433.
Levine, B., Kroemer, G., 2008. Autophagy in the pathogenesis of disease. Cell 132(1), 27–42.